



1 Riverine phosphorus gain and loss across the conterminous United 2 States

3 Yiming Wang¹, Xuesong Zhang², Kaiguang Zhao¹, Robert D. Sabo³, Yuxin Miao⁴, Christopher M. Clark³

4
5 1. Ohio Agricultural Research and Development Center, School of Environment and Natural Resources, The Ohio State
6 University, Wooster, OH 44691, USA

7 2. USDA-ARS Hydrology and Remote Sensing Laboratory, Beltsville, MD, 20705-2350, USA

8 3. United States Environmental Protection Agency, Office of Research and Development, Center for Public Health and
9 Environmental Assessment, Health and Environmental Effects Assessment Division, Washington, DC, 20460, USA.

10 4. Precision Agriculture Center, Department of Soil, Water and Climate, University of Minnesota, St. Paul, MN 55108, USA

11

12 *Correspondence to:* Yiming Wang (wang.20415@osu.edu); Xuesong Zhang (Xuesong.Zhang@usda.gov)

13 **Abstract.** Excess riverine phosphorus represents a preeminent catalyst for water quality degradation. Spatial mapping and
14 characterization of the net gain and loss of riverine phosphorus help discern the critical source areas. Here, we developed a
15 dataset encompassing phosphate (PO_4^{3-}) and total phosphorus (TP) gain and loss across catchments in the conterminous United
16 States (CONUS). We compiled 51,394 PO_4^{3-} and 285,675 TP concentration data points and estimated PO_4^{3-} and TP loads at
17 963 and 2,317 stations, respectively. Next, we leveraged the upstream-downstream topology information from the National
18 Hydrography Dataset Plus (NHDPlus) catchment map at the Hydrologic Unit Catalogue-12 (HUC12) level to derive the net
19 gain and loss of riverine phosphorus across catchments in the CONUS. Such maps can be used to estimate potential
20 contributions of point and non-point sources to riverine phosphorus pollution at refined spatial scales, identify different major
21 factors controlling local riverine P gain and loss compared to P loads, and evaluate watershed model's fidelity for representing
22 riverine P cycling. The resultant dataset is provided in Excel (.xlsx) format, accessible at Figshare
23 (<https://doi.org/10.6084/m9.figshare.28509317>, Wang et al., 2025). Leveraging the HUC12 information for spatialization, the
24 new datasets aim to address the existing gap in regional characterization of riverine phosphorus and support effective
25 management practices across the CONUS.



26 1 Introduction

27 Eutrophication is a widespread water quality challenge across the globe, with significant economic cost (e.g., \$1 billion in
28 Europe and \$2.2 billion annually in the United States (U.S.)) (Wurtsbaugh et al., 2019). Excess phosphorus (P) is a primary
29 contributor to eutrophication in streams and rivers, especially in intensive agricultural regions (Brownlie et al., 2022; Royer et
30 al., 2006a). Riverine export of P is also a major contributor to oxygen-depleted dead zones in coastal waters, causing damage
31 to underwater life (Diaz and Rosenberg, 2008). There is an urgent need for global actions to reduce P pollution for the
32 environment and human health (UNEP, 2025).

33 Nonpoint or diffuse sources, particularly nutrients applied to agroecosystems, are often recognized as the primary source of
34 water pollution (Carpenter et al., 1998). P surplus in agricultural soils due to excessive fertilization and manure application
35 can be transported to water bodies through surface runoff and groundwater pathways, and cause persistent water pollution
36 (Stackpoole et al., 2019). The diffuse nature of nonpoint source pollution poses challenges for directly identifying and
37 regulating critical source areas. Existing riverine P pollution databases mainly focus on certain agricultural areas (Ringeval et
38 al., 2024). Given the considerable spatial variation in P inputs to rivers (Arheimer and Lidén, 2000; Stackpoole et al., 2019;
39 Zhang et al., 2017), there is a lack of large-scale riverine P datasets at sufficient spatial scales across the conterminous United
40 States (CONUS) to quantify and analyze riverine P gain and loss. Such datasets, in conjunction with other observed and
41 modelled P data (e.g., point source discharge) help identify regions with high non-point source P inputs, thereby supporting
42 more effective targeting of measures for P pollution control. In addition, the datasets can also be used to assess fidelity of
43 distributed watershed models and understand key factors influencing local riverine P cycling.

44 In this study, we aim to develop new datasets for spatial characterization of riverine P gain and loss across the CONUS, to
45 help identify critical source areas and improve prioritization and implementation of nutrient management activities. The
46 subsequent sections of this paper include the method used to generate spatial riverine P gain and loss (Section 2), results
47 detailing the P dataset (Section 3), discussion of influencing factors and potential uncertainties (Section 4), codes and data
48 availability (Section 5), and conclusions (Section 6).

49

50 2 Materials and Methods

51 2.1 Overview

52 To estimate riverine P gain and loss data across the CONUS, we compiled streamflow and P concentration data (i.e., unfiltered
53 phosphate (PO_4^{3-})) and total phosphorus (TP) at over 1,000 hydrological stations in the CONUS and calculated P loads at those
54 stations using the Load Estimator (LOADEST) program (Runkel et al., 2004) (Fig. 1). Next, we estimated P gain and loss
55 across the catchments measured by one downstream station and its immediate upstream stations using the upstream-
56 downstream connectivity information contained in the National Hydrography Dataset Plus (NHDPlus) catchments



(https://nhdplus.com/NHDPlus/NHDPlusV2_data.php), resulting in 547 and 1,225 unique Hydrologic Unit Catalogue (HUC) groups for PO_4^{3-} and TP, respectively. Each HUC group has a unique pair of downstream and upstream stations that allows us to calculate the gain and loss of riverine P (as illustrated in Fig. S1 in the Supplemental Information). Note that headwater HUC groups only have one downstream station without upstream stations draining to them. Due to differences in data availability, the riverine PO_4^{3-} and TP gain and loss data cover 52,020 and 65,735 Hydrologic Unit Catalogue-12 (HUC12) catchments, respectively. Then we estimated potential contribution to P pollution from nonpoint sources by subtracting upstream P inputs and point source P inputs from the riverine P gain and loss in each catchment. Finally, we used land cover and climate data to evaluate major controls of riverine P gain and loss.

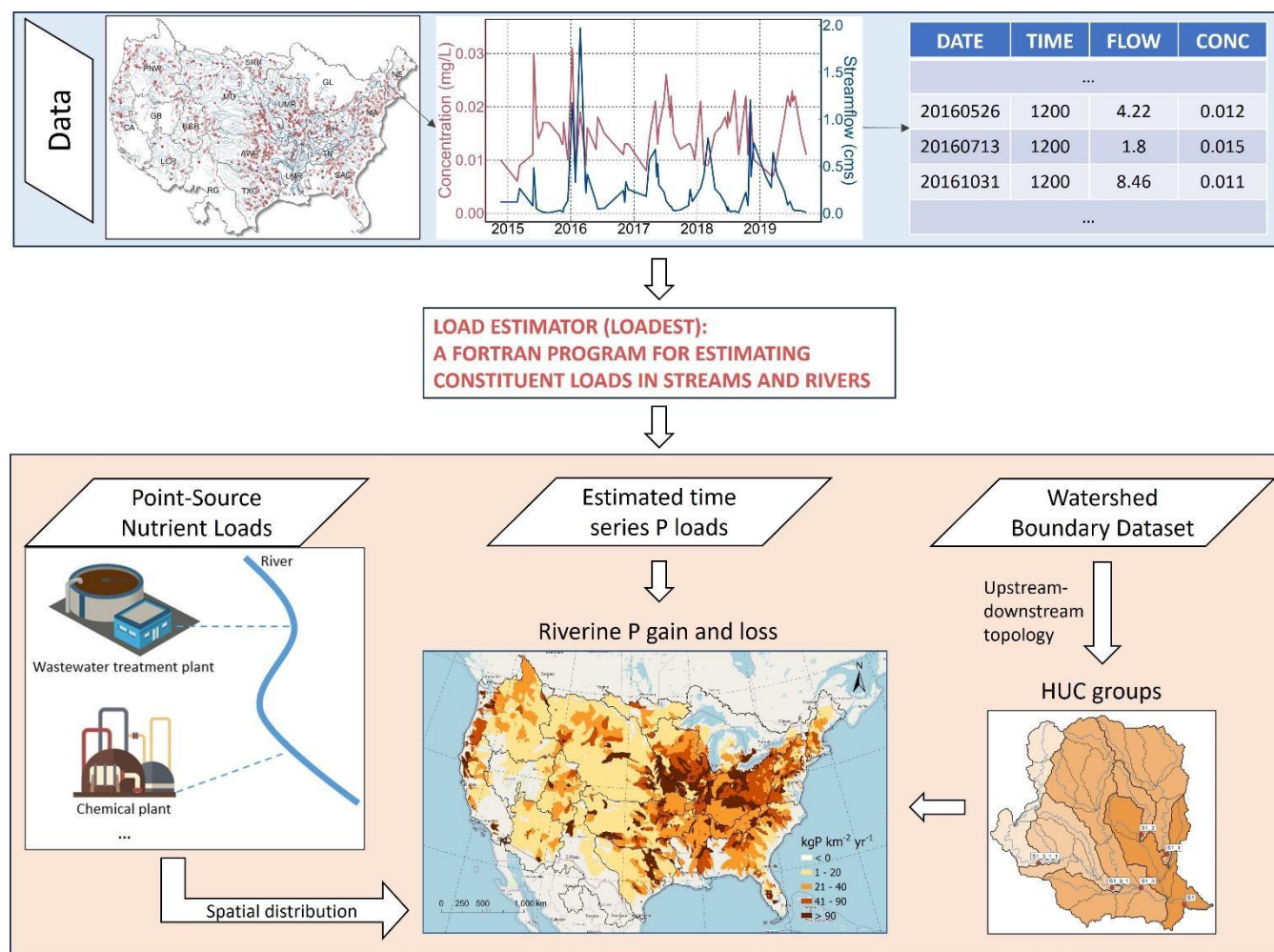


Figure 1: Overview of the generation of TP and PO_4^{3-} gain and loss data across the CONUS. A more detailed description and higher resolution figure about HUC group generation can be found in Text S2 and Fig. S1.



68 2.2 Study area

69 The CONUS (i.e., the lower 48 states of the U.S.) is located in North America from $98^{\circ} 34'$ to $46^{\circ} 20'$ W longitude and from
70 $39^{\circ} 49'$ to $41^{\circ} 43'$ N latitude, covering an area of 8,080,464.3 km² with a north-to-south distance of approximately 2,660 km.
71 The terrain features higher elevations in the west and flatter areas in the east. Based on the Watershed Boundary Dataset (WBD;
72 <https://water.usgs.gov/GIS/huc.html>), the CONUS includes 18 major watersheds, encompassing several large rivers such as
73 the Mississippi and Colorado Rivers.

74 2.3 Data compilation

75 We compiled 51,394 PO₄³⁻ (USGS parameter code 00650) concentration data from 963 hydrological stations (spanning from
76 1952 to 2022) and 285,675 TP (USGS parameter code 00665) observations from 2,317 hydrological stations (spanning from
77 1958 to 2023) across the CONUS from the Water Quality Portal (Read et al., 2017). For each P observation, we identified co-
78 located hydrological stations (Wang, Zhang, Zhao, et al., 2024) and downloaded and processed daily streamflow data from the
79 U.S. Geological Survey (USGS) National Water Information System. We calculated an average P concentration where there
80 were multiple P concentration observations on the same day. Before calculating the P load at a hydrological station with the
81 LOADEST model, we excluded stations with less than 12 data points. Thus, we finally selected 547 stations for PO₄³⁻ and
82 1,225 stations for TP. For TP, the "Point-Source Nutrient Loads to Streams of the Conterminous United States" dataset provides
83 estimated point-source inputs at the HUC12 level (Skinner and Maupin, 2019). This allowed us to aggregate the total TP input
84 to rivers for the catchments used to calculate riverine TP gain and loss. Note that the point source dataset does not contain
85 PO₄³⁻.

86 Land cover and climatic controls of riverine P gain and loss were also assessed. Land cover data were derived from the National
87 Land Cover Database (NLCD; <https://doi.org/10.5066/P94UXNTS>), which provided long-term average information on
88 various land cover types: barren land, crops, forest, hay, herbs, impervious surfaces, scrub, water, herbaceous wetlands, and
89 woody wetlands (Homer et al., 2012). Climate data were sourced from the PRISM dataset
90 (<https://www.prism.oregonstate.edu/>), including annual average temperature and total precipitation (Page et al., 2021). Using
91 upstream-downstream topology information, we calculated the total area of each land cover type from the headwater to the
92 current catchment at the HUC12 scale, representing their cumulative impact. For climate data, the local climate within each
93 HUC12 was used. The P surplus was accessed from the National Inventory of Phosphorus (NIP), which provides major inputs
94 and outputs of reactive P at the HUC8 scale across the CONUS (Sabo et al., 2021).

95 2.4 Riverine P gain and loss across catchments in the CONUS

96 Riverine P gain and loss was estimated by calculating the difference between P loads at a downstream hydrological station and
97 the sum of P loads from its neighbouring upstream stations. For multiple USGS stations located in the same HUC12 catchment,
98 we kept only one station on the mainstem of the river that is closest to the outlet of the HUC12 catchment, by comparing the



99 drainage area of the gaging station and the HUC12 catchment in which it is located. For headwaters, since there are no upstream
100 gages, the P load was used as the net riverine gain. The upstream-downstream topology relationship between the hydrological
101 stations was derived from the HUC12 catchments from the watershed boundary dataset (WBD;
102 <https://water.usgs.gov/GIS/huc.html>). Such a method has been outlined and tested by Qiu et al. (2023) (Text S2). As explained
103 above, we identified 547 and 1,225 unique HUC groups for PO_4^{3-} and TP, respectively. Note that each HUC group includes
104 multiple HUC12 polygons and these HUC12 catchments share the same gain and loss data.

105 For each HUC group, the balance of riverine P can be expressed as follows:

$$\begin{aligned} 106 \quad P \text{ load at downstream outlet} &= (P \text{ loads from upstream inputs}) + (P \text{ from point sources}) - \\ 107 \quad & (Riverine removal of P from point sources) + (P \text{ from non-point sources}) - \\ 108 \quad & (Riverine removal of P from non-point sources) \end{aligned} \quad (1)$$

109 Rearranging the above equation leads to:

$$\begin{aligned} 110 \quad (P \text{ from nonpoint sources}) &= P \text{ gain and loss} - (P \text{ from point sources}) + \\ 111 \quad & (Riverine removal of P from point sources) + (Riverine removal of P from non-point sources) \end{aligned} \quad (2)$$

112 where $P \text{ gain and loss} = (P \text{ load at downstream outlet}) - (P \text{ loads from upstream inputs})$.

113 Given that rivers often remove a small portion of P load (e.g., 12%) (Maavara et al., 2015), we assumed that
114 $(P \text{ from nonpoint sources}) = P \text{ gain and loss} - (P \text{ from point sources})$ is a lower-end estimate of the nonpoint
115 source contribution to riverine P for each HUC group. Since only TP from point sources is available, we derived nonpoint-
116 source TP loads but not for PO_4^{3-} .

117 2.5 Evaluation of estimated riverine load

118 We evaluated the consistency of the PO_4^{3-} and TP loads against another independent dataset derived with the Weighted
119 Regressions on Time, Discharge, and Season (WRTDS) model (Hirsch et al., 2010; Zhang and Hirsch, 2019). First, we
120 compared multi-year average TP loads from 151 hydrological stations. We also evaluated the estimated unfiltered PO_4^{3-} loads,
121 which assess the mass of reactive P susceptible to being released in the water column under various redox conditions.
122 Furthermore, the reliability of the upstream-downstream connectivity information is important for deriving the drainage area
123 of HUC groups that are controlled by pairs of upstream and downstream hydrological stations. Here we used a quality-checked
124 and corrected NHDPlus HUC12 catchment map (Wang, Zhang, & Zhao, 2024) that has been verified for reliably deriving the
125 drainage area of each USGS hydrologic station as compared to the USGS GAGES-II reported values (Falcone and Survey,
126 2011). These efforts helped ensure the quality of the riverine P gain and loss data developed in this study.

127 2.6 Analysis of environmental controls

128 Recent studies reveal that shifts in land use, agricultural practices, and climatic conditions have introduced a pervasive increase
129 in soluble P concentrations across many different watersheds (Houser and Richardson, 2010; Singh et al., 2023). To assess the



130 spatial factors influencing riverine P gain and loss, we employed random forest modelling to evaluate the relative importance
131 of multiple environmental variables (Breiman, 2001). These factors were categorized into three groups: climatic factors, land
132 cover types, and additional influences such as cumulative agricultural inputs and upstream loads. Given that the NIP dataset is
133 only available at the HUC8 scale and some HUC groups are larger than the HUC8 catchment areas, we calculated the
134 cumulative agricultural inputs at the HUC4 scale. In more detail, we used the ranger package, optimizing the model structure
135 with the caret package in R. Key tuning parameters included the number of variables to use in each split (mtry), the number of
136 trees (n_trees) and the minimum size of data points before splitting a tree (min_n). The tuning process was performed by doing
137 a grid search for mtry (2-6) and min_n (10-20), then a second search was performed to find the optimal n_trees parameter
138 (500-3000). To minimize random effects, the model was run 10 times, and we calculated the average importance value and
139 harmonic mean p-value (Wilson, 2019).

140 3 Results

141 3.1 Riverine phosphorus data

142 We created two datasets, "Riverine PO₄³⁻" and "Riverine TP," that encapsulate estimated multi-year average riverine gain and
143 loss and loads, as well as point source and nonpoint source contributions for each HUC group for PO₄³⁻ and TP, respectively
144 (Table 1). Complementing this information, the datasets encompass the location (i.e., longitude and latitude) of the outlet of
145 the HUC group, the area of the HUC group, the count of observations used to calculate P loads, and commencement and
146 termination years of observed data, to facilitate user-defined subsetting of the datasets. Additional information regarding the
147 regression model is also included, such as the form of the regression model selected by LOADEST and the associated
148 coefficient of determination (r²) values.

149 Across the board, the average r² values for the best-fit model (Table S1) across all sites are 0.76 for PO₄³⁻ loads and 0.83 for
150 TP loads. It is noteworthy, however, that certain hydrologic stations exhibited low r² values due to the limited availability of
151 paired P concentration with streamflow data for regression.

152

153 **Table 1. Data records in the "Riverine PO₄³⁻" and "Riverine TP" datasets.**

Field name	Description
Station ID	U.S. Geological Survey designated ID; Note that this ID is also used to denote a unique HUC group
Lat	Latitude of the hydrologic station at the outlet of a HUC group
Long	Longitude of the hydrologic station at the outlet of a HUC group
Area	Area of the HUC group
Load	The amount of PO ₄ ³⁻ or TP loads at the outlet hydrologic station of a HUC group (kgP yr ⁻¹)

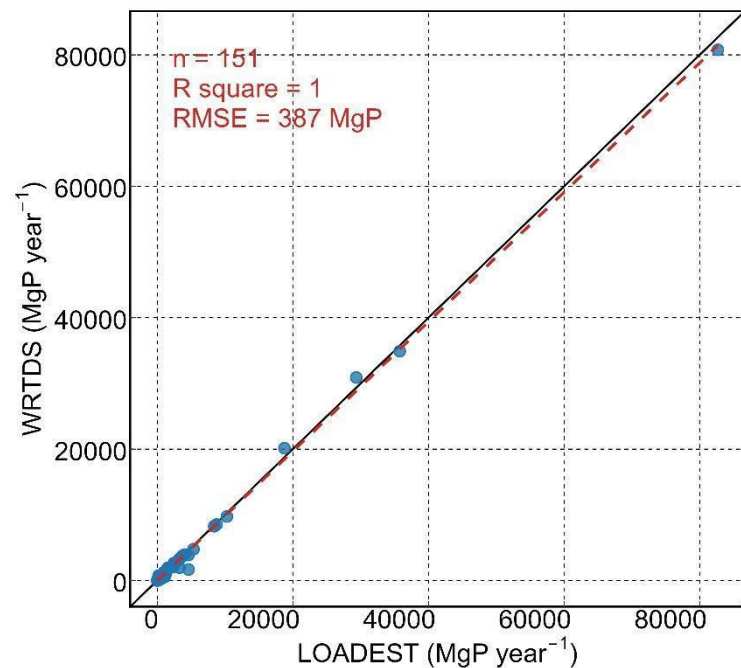


P gain and loss	The difference between P loads at the outlet of a HUC group and all its immediate upstream stations $(\text{kgP km}^{-2} \text{ yr}^{-1})$
NonPts TP contribution*	Nonpoint-source contribution to riverine phosphorus from a HUC group $(\text{kgP km}^{-2} \text{ yr}^{-1})$
Pts TP load	Point-source TP loads (kg yr^{-1}) from a HUC group
obsNum	The number of phosphorus concentration data with paired streamflow data
startYr	The starting year of the observed data
endYr	The ending year of the observed data
modelID	The ID of regression model used for load estimation
r2	R-Squared (%) for the selected LOADEST regression model used to estimate the P load

154 Note: * only for TP as only point source TP inputs are available.

155

156 Our TP load estimates are highly consistent with the WRTDS model with high r^2 and low root mean square error (RMSE)
 157 (Fig. 2). The minor disparities observed between these two datasets are likely attributable to variations in temporal coverage.
 158 For PO_4^{3-} , we found that only 11 stations with WRTDS estimates matched the stations used here, and all 11 stations are
 159 located in small watersheds. Therefore, we leveraged filtered PO_4^{3-} loads estimated by WRTDS to assess if the LOADEST
 160 estimated unfiltered PO_4^{3-} loads. Unfiltered PO_4^{3-} measures both the dissolved PO_4^{3-} as well as PO_4^{3-} compounds bound to
 161 suspended sediments and organic materials, and thus will have higher load compared to filtered PO_4^{3-} measurements (Fig.
 162 S2). Nonetheless, the high correlation indicates our estimates of unfiltered PO_4^{3-} are reasonable.



163



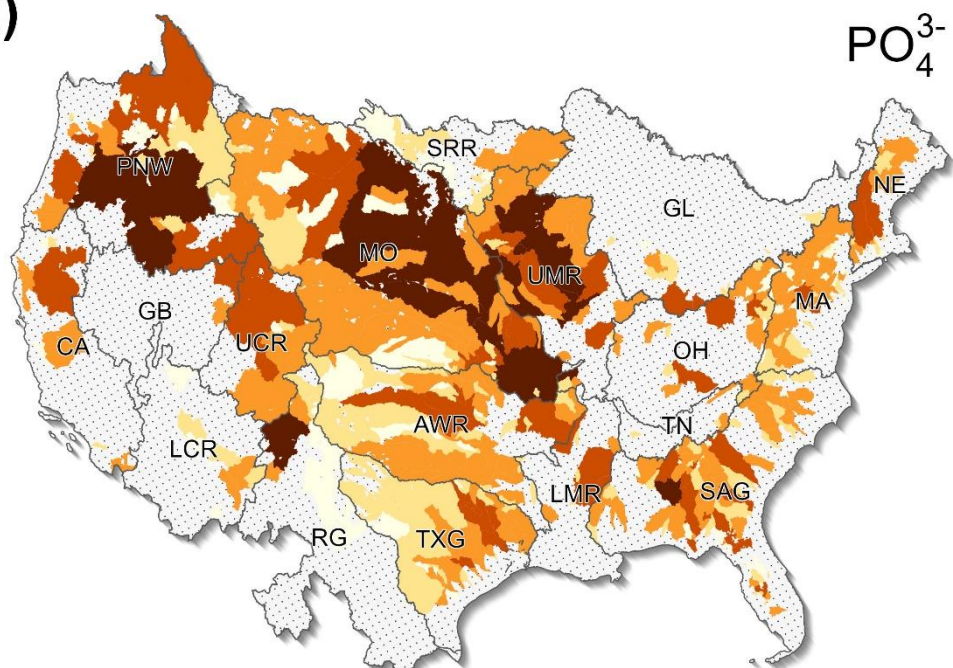
164 **Figure 2: Comparison of riverine TP loads between our estimates and previous WRTDS estimated values at 151 hydrological
165 stations. Note that the riverine TP loads vary greatly at different locations and over time, with most sites being below 10,000 MgP
166 year⁻¹.**

167 Spatial patterns of PO₄³⁻ and TP loads from each HUC group across the CONUS are shown in Fig. 3. Additionally, the location
168 of the hydrologic station at the outlet of each HUC group and the loads of streams in which it is located are shown in Fig. S3.
169 The datasets encompass 547 hydrologic stations/HUC groups for PO₄³⁻ and 1,225 stations/HUC groups for TP, covering
170 4,894,464 and 6,118,360 km² PO₄³⁻ and TP, respectively. The difference in spatial coverage is mainly due to the abundance of
171 TP compared to PO₄³⁻. Stations with high P loads are predominantly situated in the Midwest or proximate to megacities, with
172 a general pattern of higher P loads observed in the eastern U.S. PO₄³⁻ loads range from 111 to 31,671,885 kgP yr⁻¹ and TP
173 loads range from 235 to 336,223,136 kgP yr⁻¹. Median loads are 76,202 and 108,305 kgP yr⁻¹ and average loads are 436,311
174 and 1,012,363 kgP yr⁻¹, for PO₄³⁻ and TP, respectively.



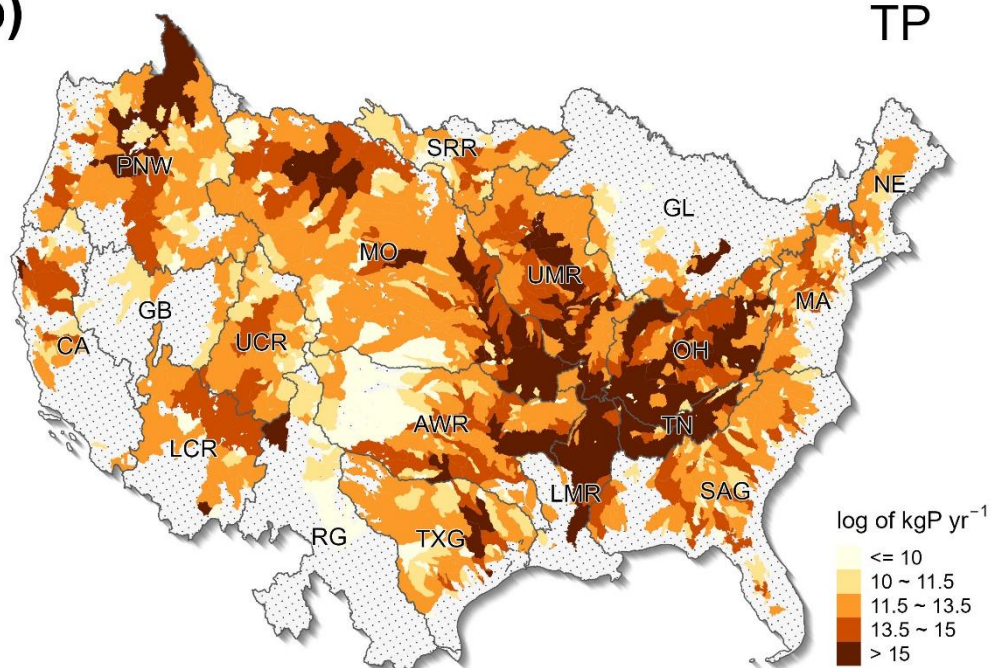
(a)

PO_4^{3-}



(b)

TP





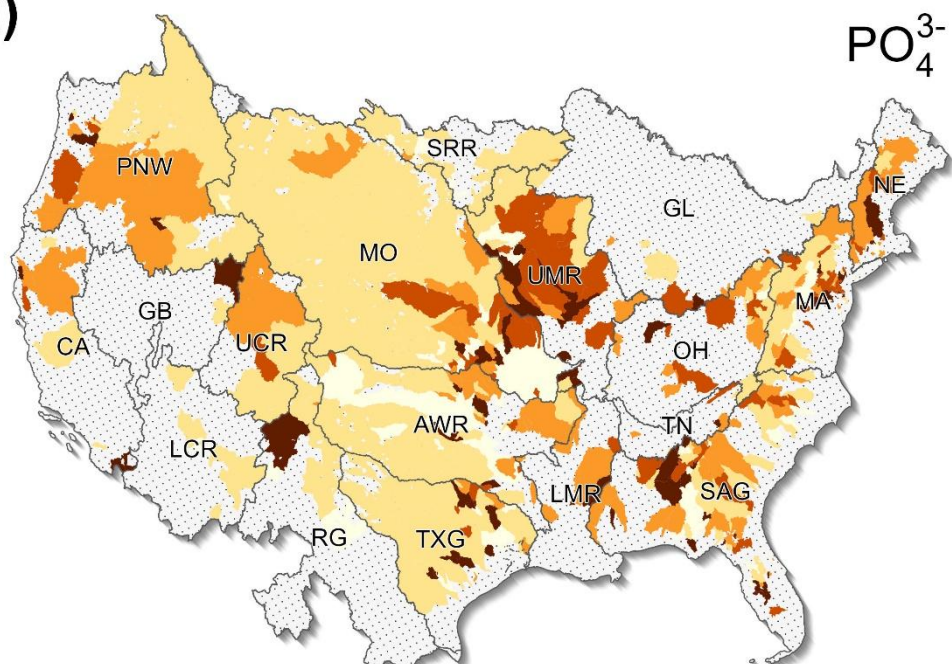
176
177
178 **Figure 3: Riverine (a) PO_4^{3-} and (b) TP loads from HUC groups across the CONUS. The boundary lines show the Hydrologic Unit
Catalogue 2-digit (HUC2) watersheds. Grey areas indicate regions with no data. For visualization purposes, the logarithm was used
here.**

179
180 The spatial distribution of riverine P gain and loss is shown in Fig. 4. Both PO_4^{3-} and TP gain and loss exhibit similar spatial
181 patterns over the CONUS, with most areas exhibiting riverine P gains. The area-weighted average PO_4^{3-} gain stands at 25.39
182 $\text{kgP km}^{-2} \text{ yr}^{-1}$, and the TP gain is $33.68 \text{ kgP km}^{-2} \text{ yr}^{-1}$. Median PO_4^{3-} and TP gains are lower than averages, standing at 16.75
183 $\text{kgP km}^{-2} \text{ yr}^{-1}$ and $33.57 \text{ kgP km}^{-2} \text{ yr}^{-1}$, respectively. At the HUC group scale, the highest area-weighted PO_4^{3-} gain was
184 identified in the Upper Mississippi Region (UMR), amounting to about $113.96 \text{ kgP km}^{-2} \text{ yr}^{-1}$. The highest TP gain reached
185 $186.55 \text{ kgP km}^{-2} \text{ yr}^{-1}$ in the Tennessee Region (TN). Notably, widespread regions in the Midwest exhibit heightened P gains,
186 particularly in terms of PO_4^{3-} , suggesting a discernible impact of human activities (e.g., agricultural fertilization). At the HUC2
187 level, the lowest area-weighted PO_4^{3-} gain ($1.72 \text{ kgP km}^{-2} \text{ yr}^{-1}$) was found in the Rio Grande Region (RG), and the lowest TP
188 gain ($0.62 \text{ kgP km}^{-2} \text{ yr}^{-1}$) was found in the Upper Colorado Region (UCR). Refined examination at the HUC group level
189 showed that, over the CONUS, $392,778 \text{ km}^2$ and $1,468,973 \text{ km}^2$ areas exhibited riverine PO_4^{3-} and TP losses, respectively.
190



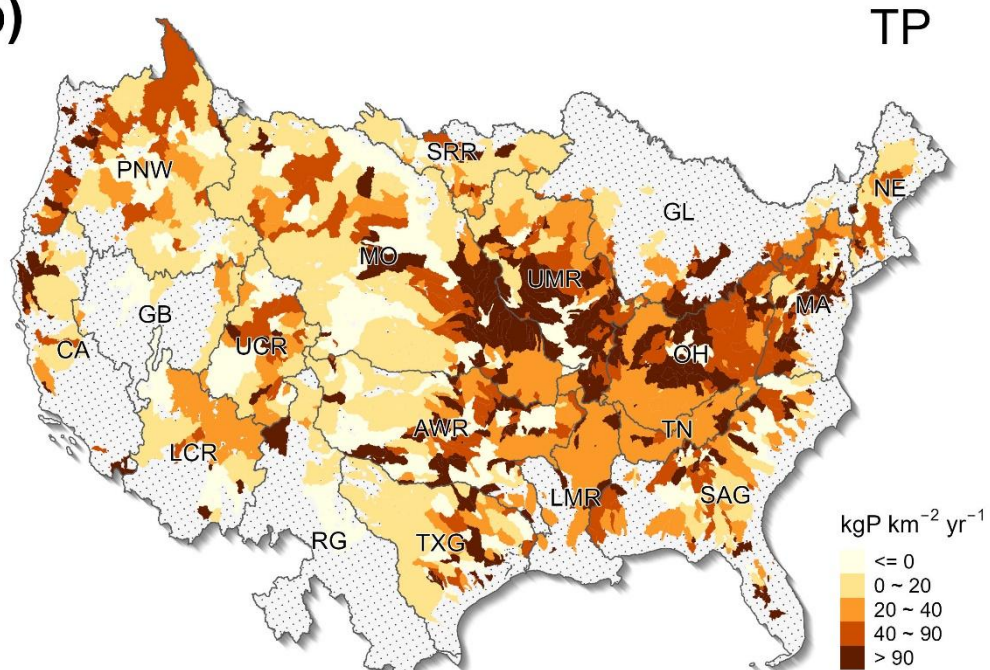
(a)

PO_4^{3-}



(b)

TP





192 **Figure 4: The spatial distribution of the gain and loss in riverine (a) PO_4^{3-} and (b) TP over the CONUS. The boundary lines show**
193 **the Hydrologic Unit Catalogue 2-digit (HUC2) watersheds. Grey areas indicate regions with no data.**

194

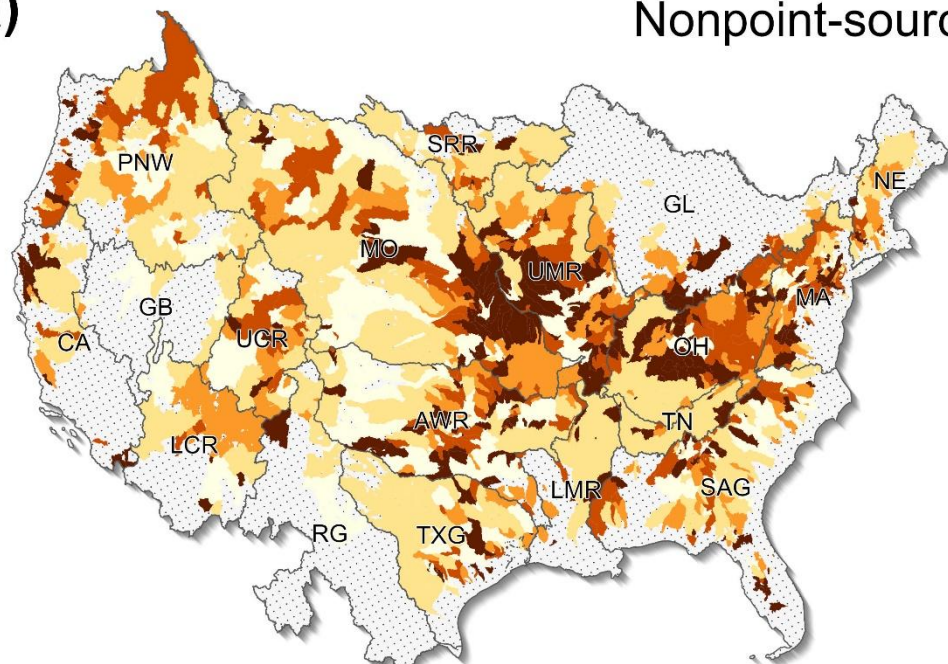
195 **3.2 Point and nonpoint source contributions**

196 We also mapped the spatial point source and nonpoint source inputs of TP, as shown in Fig. 5. The nonpoint source
197 contributions are estimated based on Equation (2), which provides a lower-end estimate given that the riverine removal of
198 point and nonpoint source P as shown in Equation (2) was not considered. Point and nonpoint source contributions to riverine
199 TP pollution exhibited large differences in both the magnitude and spatial distribution. Over the CONUS, the area-averaged
200 point source input of TP is $5.44 \text{ kgP km}^{-2} \text{ yr}^{-1}$. By subtracting point source inputs from the calculated TP gain and loss, we
201 obtained an area-averaged nonpoint source TP contribution of $28.24 \text{ kgP km}^{-2} \text{ yr}^{-1}$. Regions characterized by high TP gain with
202 minimal point source pollution were observed in the Midwest. Notably, in most of the agriculturally intensive Missouri and
203 Tennessee-Ohio river basins, total nonpoint source discharge significantly surpassed point source contributions. Upon the
204 exclusion of point source contributions (Fig. 5b), there is a substantial change, with the areas with riverine TP losses expanding
205 to $1,603,258 \text{ km}^2$, most of them in the Missouri and Arkansas-White-Red River Basins. In general, most watersheds with
206 negative nonpoint sources are concentrated in the western U.S. This does not mean that the nonpoint source P inputs are
207 negative, but indicates that riverine processes likely removed a large fraction of point and nonpoint source P.



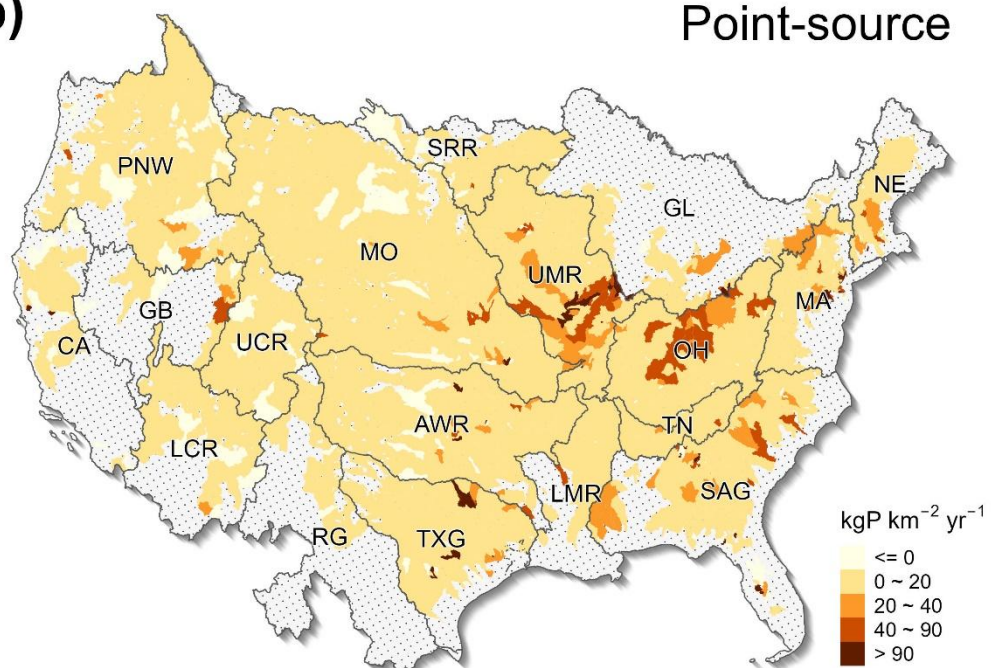
(a)

Nonpoint-source



(b)

Point-source



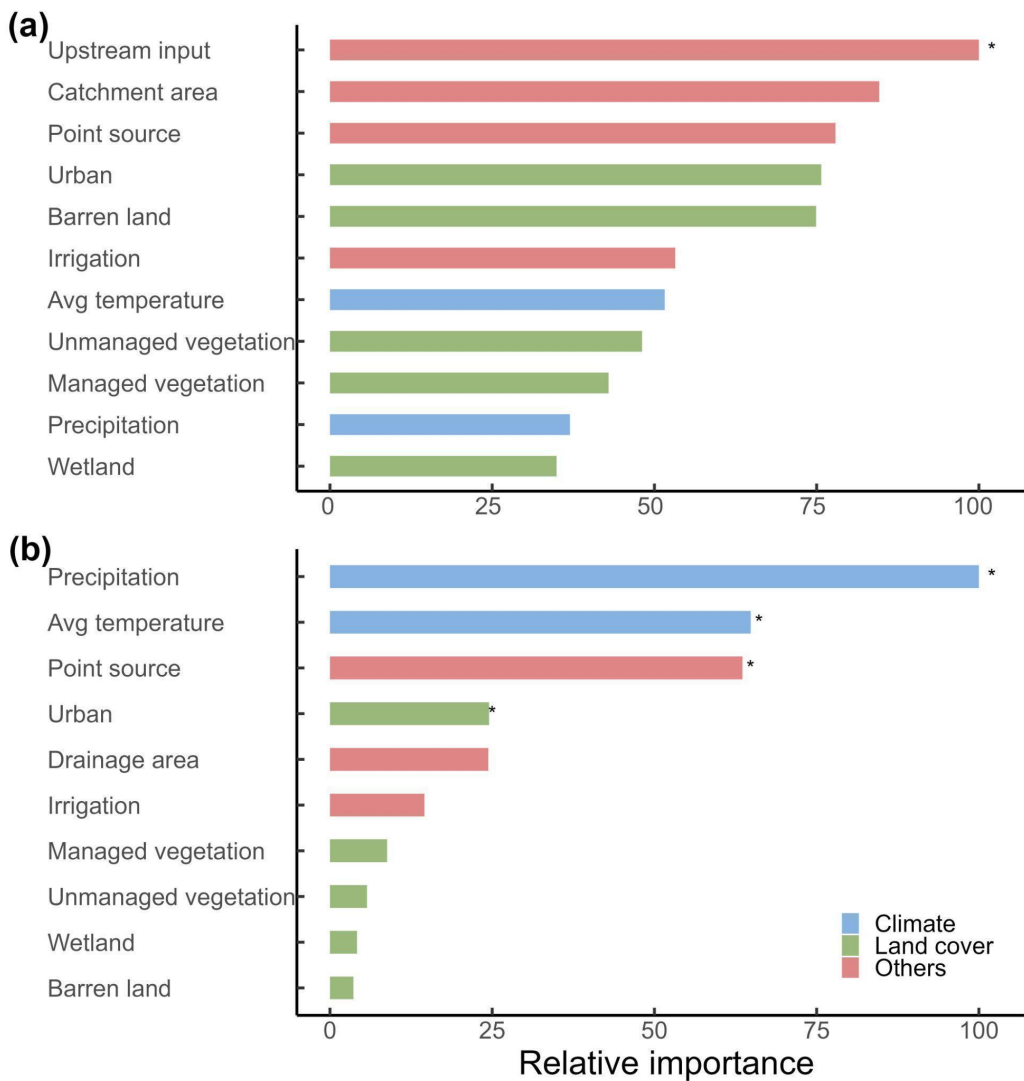


209 **Figure 5: The spatial distribution of (a) nonpoint source and (b) point source contributions to riverine P pollution over the CONUS.**
210 **The boundary lines show the Hydrologic Unit Catalogue 2-digit (HUC2) watersheds. Grey areas indicate regions with no data.**

211

212 **3.3 Factors influencing TP**

213 We employed a random forest model to assess the influence of climate, land use, human activities, and catchment
214 characteristics on riverine TP gain and loss and TP loads (Fig. 6). Note that the calculated P loads represent the outcome of
215 the entire upstream catchment processes, while the riverine P gain and loss data represent both upstream catchment processes
216 (e.g., P inputs from upstream) and local catchment properties (e.g., climate and land use in a HUC group). Such differences
217 lead to the use of different sets of influencing factors (Fig. 6). The land use, climate and point source factors were calculated
218 for the entire upstream area draining to a hydrological station for TP load analysis. In contrast, those factors were averaged
219 over a HUC group for riverine gain and loss analysis. Additionally, for the analysis of riverine P gain and loss data, we included
220 upstream P inputs. Analysis results indicate that upstream input is the sole statistically significant factor affecting TP gain and
221 loss, with climate and land cover showing no notable impact. Conversely, TP loads are predominantly influenced by climatic
222 factors, alongside significant contributions from point source discharges and urban land use.



223

224 Figure 6: The importance of factors influencing (a) TP gain and loss and (b) TP loads. Asterisks indicate significance at a level of
225 0.05.

226 4 Discussion

227 4.1 Important contributions from nonpoint sources to riverine P pollution

228 The estimated area-averaged nonpoint source TP contribution ($28.24 \text{ kgP km}^{-2} \text{ yr}^{-1}$) represents a reduction of 16.2% from the
229 calculated TP gain and loss that includes contributions from both point and nonpoint sources ($33.68 \text{ kgP km}^{-2} \text{ yr}^{-1}$). Given that
230 the TP inputs from point and nonpoint sources are often subject to riverine removal (Maavara et al., 2015), the estimated
231 nonpoint source TP based on Equation (1) should be augmented by the amount of total TP inputs (including both nonpoint and
232 point source) removed through riverine processes. Therefore, the calculated nonpoint source inputs of TP represent an



233 underestimate of the contributions from nonpoint sources. If we assume a 12% removal rate for TP inputs (Maavara et al.,
234 2015), then the nonpoint source inputs of TP would increase from $28.24 \text{ kgP km}^{-2} \text{ yr}^{-1}$ to $32.28 \text{ kgP km}^{-2} \text{ yr}^{-1}$. Collectively, the
235 results show that the nonpoint sources likely contribute more than 84% of riverine TP pollution.

236 **4.2 Implications for analysing environmental controls of riverine P**

237 Climatic factors were key drivers of TP loads at the outlet of a watershed, which in general aligns with findings from previous
238 studies (Sabo et al., 2023) and underscores the role of climate in nutrient transport dynamics. Our environmental control
239 analysis using the gain and loss data showed that upstream inputs are leading control of local riverine gain and loss (Fig. 6a),
240 in addition to local inputs of P from point and nonpoint sources and local riverine processes, such as in-stream retention through
241 mechanisms such as P absorption by periphyton via photosynthesis and hydrological processes like reduced streamflow and
242 sedimentation (Dodds, 2003; Withers and Jarvie, 2008). Notably, although accumulated agricultural P inputs (i.e., livestock
243 waste and agricultural fertilizer) positively influenced TP gain and loss (Fig. S4), they were not included in this analysis due
244 to mismatch of spatial scales. In general, using TP loads and riverine P gain and loss can lead to pronounced differences in the
245 analysis of importance of environmental controls. Although climate conditions (i.e., precipitation and temperature) are the
246 major controls of TP loads, which represent the integration of the entire watershed conditions, while riverine P gain and loss
247 indicate that the amount of upstream P inputs entering a local catchment is an important factor influencing the riverine
248 processing of P.

249 Both the differences and the analysis using TP loads and riverine gain and loss data revealed the importance of urban land and
250 agricultural management. For example, both analyses show that irrigation can influence riverine TP, indicating that improving
251 irrigation efficiency and technology holds potential to reduce TP inputs from cropland fertilization (Xia et al., 2020). Though
252 we didn't assess factors influencing PO_4^{3-} due to the lack of point source PO_4^{3-} data, TP hotspots are expected to occur further
253 downstream than PO_4^{3-} hotspots (Fig. 3). This is probably because rivers typically can retain (e.g., periphyton assimilation,
254 adsorption onto suspended or bed sediment) a considerable proportion of incoming soluble-reactive P (e.g., PO_4^{3-}) within the
255 upper network, whereas particulate P continue to transport to downstream (Jarvie et al., 2012; Robertson and Saad, 2019;
256 Royer et al., 2006b). Overall, the intricate interplay between climate and land use factors underscores the complex nature of P
257 dynamics in riverine systems. These newly developed riverine gain and loss datasets help improve understanding of local
258 controls of riverine P dynamics and identify hotspots of changes in riverine P.

259 **4.3 Limitations and contribution**

260 While the newly developed datasets leverage upstream-downstream topology information at the HUC12 level to help increase
261 the spatial resolution of riverine P gain and loss data, it is essential to acknowledge limitations relevant to understanding and
262 quantifying P cycles and identifying sources of P inputs. First, the accuracy of load estimation via LOADEST is contingent
263 upon the availability of paired P concentration data from hydrological stations. Stations with limited observations may



264 introduce higher uncertainties in load estimations. The robustness of our datasets is partially reflected in the number of
265 observations available. The average and median numbers of PO_4^{3-} observations per site is 54 and 29, respectively; for TP, the
266 average and median numbers of observations per site is 134 and 90, respectively. In addition, the average center year of TP
267 observations is 1992, with a median of 1991, while for PO_4^{3-} , the overall observation time is relatively early, with an average
268 of 1981 and a median of 1980. The use of AIC to choose the most parsimonious regression model (average r^2 of 0.76 and 0.83
269 for PO_4^{3-} and TP, respectively) helped reduce uncertainties in load estimates.

270 Additionally, we calculated the P loads by averaging over different time periods with available data for each hydrological
271 station. The mismatch between observational periods of upstream and downstream hydrological stations could introduce
272 uncertainties, given that the available data cover various time periods for different hydrological stations. For example,
273 streamflow discharge, which is important for calculating nutrient loads, can vary from year to year. Here, we assumed that
274 multi-year average estimates of P loads are representative of the long-term pattern at a hydrological station. This may not hold
275 for some upstream and downstream stations covering time periods that do not overlap with each other. Therefore, we provided
276 the number and period of observations and model performance information in the datasets, which can help users to refine the
277 calculation of riverine P gain and loss by further screening the P loads data at the hydrological stations. Note that available
278 hydrologic stations with observed P concentration and streamflow data are relatively sparse in the western vs. eastern U.S.,
279 particularly for PO_4^{3-} . This led to large gaps in the spatial coverage of the datasets (Fig. 4). Increasing the number of
280 hydrological stations with P observations holds the potential to enhance the accuracy of riverine P estimates in the future.

281 It is also worth noting that the calculated contribution of TP from nonpoint sources represents a conservative estimate, given
282 the unknown rate of TP removal from point and nonpoint sources. Although previous studies showed that TP removal rates
283 were generally small, they could vary substantially across regions, as evidenced by the areas with riverine P loss (Fig. 4). It is
284 reasonable to assume that the estimated TP contribution from nonpoint sources is greater than 84% over the CONUS; however,
285 the local TP contribution from nonpoint sources could be much lower, particularly in regions with high point source inputs.
286 Also, the removal rates of P from point and nonpoint sources are likely different due to differences in the quality of P inputs
287 (e.g., biodegradability and adsorption and desorption to sediments) and flow pathways (Wang et al., 2025). Therefore, caution
288 should be taken when interpreting the local contribution to P pollution from nonpoint sources.

289 Despite these challenges, our datasets make a unique contribution to the quantification and analysis of riverine P load, gain
290 and loss, and sources across the CONUS. They can support the evaluation and diagnosis of large-scale watershed models, the
291 examination of environmental controls on riverine P loads, and the estimation of contributions to P gain and loss. The insights
292 derived from our datasets contribute to a more comprehensive understanding of P dynamics, providing a foundation for
293 improved water quality management on local, regional, and national scales.



294 5 Code and data availability

295 All codes for validating and visualizing PO_4^{3-} and TP gain and loss from the load estimations were run in R version 4.3.1 and
296 are archived at https://github.com/ymwang4924/gain-loss_P. The datasets presented in the paper are available at
297 <https://doi.org/10.6084/m9.figshare.28509317> (Wang et al., 2025).

298 6 Conclusions

299 In this study, we estimated riverine loads of PO_4^{3-} and TP and derived their gain and loss across the CONUS, leveraging the
300 upstream-downstream hydrological connectivity information contained in the NHDPlus catchment map. On average, rivers
301 across the CONUS gain TP at a rate of $33.68 \text{ kgP km}^{-2} \text{ yr}^{-1}$, with notable hotspots in the Midwest. Due to the limitations of
302 data availability, the precision of estimated P gain and loss data could be influenced by the number and periods of observations
303 available at upstream and downstream stations. We provided additional information regarding the number of observations
304 available, temporal coverage of data, the regression model used, and the model's statistical performance, so that users can
305 further subset the datasets to meet certain specific criteria.

306 The riverine P gain and loss datasets allow the estimation of riverine P removal or accrual at a refined spatial resolution to
307 better reflect the impacts of local controls. In contrast, riverine P loads at hydrological stations embody the integrated processes
308 from the entire area upstream of a specific station. Also, by combining point source inputs with the riverine P gain and loss
309 datasets, we derived conservative estimates of the contribution of nonpoint sources to riverine TP ($28.24 \text{ kgP km}^{-2} \text{ yr}^{-1}$). The
310 control factor analysis with a random forest model demonstrated that upstream inputs had the greatest influence on the local
311 riverine P gain and loss, while climatic factors dominated riverine P loads at hydrological stations. This suggests that nutrient
312 management practices that prioritize enhancing irrigation efficiency and integrating strategies such as targeted fertilizer
313 application and wetland restoration may more effectively capture and reduce phosphorus mobilization from agricultural lands.
314 The newly developed riverine P datasets in this study extend utility to diverse applications, encompassing, but not limited to,
315 the evaluation of watershed models, identification of critical source areas, and optimization of agricultural management
316 strategies. Future studies may concentrate on filling gaps in the spatial and temporal coverage of the datasets (particularly for
317 PO_4^{3-}).

318 Author contributions

319 **Y.W.:** Conceptualization, methodology, investigation, formal analysis, data curation, visualization, and writing—original
320 draft. **X.Z.:** Conceptualization, methodology, investigation, writing—original draft, writing—review and editing, supervision,
321 project administration, and funding acquisition. **K.Z.:** methodology, investigation, writing—review and editing. **R.D.S.:**
322 investigation, writing—review and editing. **Y.M.:** visualization, writing—review and editing. **C.M.C.:** writing—review and
323 editing.



324 **Competing interests**

325 At least one of the (co-)authors is a member of the editorial board of *Earth System Science Data*.

326 **Disclaimer**

327 The views expressed are those of the authors, and do not necessarily represent the views or policies of the U.S. Environmental
328 Protection Agency or any other Federal agency. Any use of trade, firm, or product names is for descriptive purposes only and
329 does not imply endorsement by the U.S. Government.

330 **Financial support**

331 This research is in part supported by the U.S. Department of Agriculture – Agricultural Research Service and the National
332 Aeronautics and Space Administration (NASA 22-CMS22-0027). The mention of trade names or commercial products in this
333 publication is solely for the purpose of providing specific information and does not imply recommendation or endorsement by
334 the funding agencies.

335 **Acknowledgement**

336 We thank Sarah Stackpoole, Qian Zhang, and Kate Schofield for constructive comments and editorial suggestions on earlier
337 versions of the manuscript.

338 **References**

339 Arheimer, B. and Lidén, R.: Nitrogen and phosphorus concentrations from agricultural catchments—fluence of spatial and
340 temporal variables, *J Hydrol (Amst)*, 227, 140–159, [https://doi.org/10.1016/S0022-1694\(99\)00177-8](https://doi.org/10.1016/S0022-1694(99)00177-8), 2000.

341 Breiman, L.: Random Forests, *Mach Learn*, 45, 5–32, <https://doi.org/10.1023/A:1010933404324>, 2001.

342 Brownlie, W. J., Sutton, M. A., Heal, K. V., Reay, D. S., and Spears, B.: Our phosphorus future: towards global phosphorus
343 sustainability, 2022.

344 Carpenter, S. R., Caraco, N. F., Correll, D. L., Howarth, R. W., Sharpley, A. N., and Smith, V. H.: Nonpoint pollution of
345 surface waters with phosphorus and nitrogen, *Ecological Applications*, 8, 559–568, <https://doi.org/10.1890/1051-0761>, 1998.

346 Diaz, R. J. and Rosenberg, R.: Spreading Dead Zones and Consequences for Marine Ecosystems, *Science* (1979), 321, 926–
347 929, <https://doi.org/10.1126/science.1156401>, 2008.

348 Dodds, W. K.: The role of periphyton in phosphorus retention in shallow freshwater aquatic systems, *J Phycol*, 39, 840–849,
349 <https://doi.org/10.1046/j.1529-8817.2003.02081.x>, 2003.



350 Falcone, J. A. and Survey, U. S. G.: GAGES-II: Geospatial Attributes of Gages for Evaluating Streamflow, Reston, VA,
351 https://doi.org/10.3133/70046617, 2011.

352 Hirsch, R. M., Moyer, D. L., and Archfield, S. A.: Weighted Regressions on Time, Discharge, and Season (WRTDS), with an
353 Application to Chesapeake Bay River Inputs 1, JAWRA Journal of the American Water Resources Association, 46, 857–880,
354 https://doi.org/10.1111/j.1752-1688.2010.00482.x, 2010.

355 Homer, C. G., Fry, J. A., and Barnes, C. A.: The national land cover database, 2012.

356 Houser, J. N. and Richardson, W. B.: Nitrogen and phosphorus in the Upper Mississippi River: Transport, processing, and
357 effects on the river ecosystem, *Hydrobiologia*, 640, 71–88, https://doi.org/10.1007/s10750-009-0067-4, 2010.

358 Jarvie, H. P., Sharpley, A. N., Scott, J. T., Haggard, B. E., Bowes, M. J., and Massey, L. B.: Within-River Phosphorus Retention:
359 Accounting for a Missing Piece in the Watershed Phosphorus Puzzle, *Environ Sci Technol*, 46, 13284–13292,
360 https://doi.org/10.1021/es303562y, 2012.

361 Maavara, T., Parsons, C. T., Ridenour, C., Stojanovic, S., Dürr, H. H., Powley, H. R., and Van Cappellen, P.: Global
362 phosphorus retention by river damming, *Proceedings of the National Academy of Sciences*, 112, 15603–15608,
363 https://doi.org/10.1073/pnas.1511797112, 2015.

364 Page, M. J., Moher, D., Bossuyt, P. M., Boutron, I., Hoffmann, T. C., Mulrow, C. D., Shamseer, L., Tetzlaff, J. M., Akl, E. A.,
365 Brennan, S. E., Chou, R., Glanville, J., Grimshaw, J. M., Hróbjartsson, A., Lalu, M. M., Li, T., Loder, E. W., Mayo-Wilson,
366 E., McDonald, S., McGuinness, L. A., Stewart, L. A., Thomas, J., Tricco, A. C., Welch, V. A., Whiting, P., and Mckenzie, J.
367 E.: PRISMA 2020 explanation and elaboration: updated guidance and exemplars for reporting systematic reviews, *BMJ*, 372,
368 https://doi.org/10.1136/BMJ.N160, 2021.

369 Qiu, H., Zhang, X., Yang, A., Wickland, K. P., Stets, E. G., and Chen, M.: Watershed carbon yield derived from gauge
370 observations and river network connectivity in the United States, *Scientific Data* 2023 10:1, 10, 1–13,
371 https://doi.org/10.1038/s41597-023-02162-7, 2023.

372 Read, E. K., Carr, L., De Cicco, L., Dugan, H. A., Hanson, P. C., Hart, J. A., Kreft, J., Read, J. S., and Winslow, L. A.: Water
373 quality data for national-scale aquatic research: The Water Quality Portal, *Water Resour Res*, 53, 1735–1745,
374 https://doi.org/10.1002/2016WR019993, 2017.

375 Ringeval, B., Demay, J., Goll, D. S., He, X., Wang, Y. P., Hou, E., Matej, S., Erb, K. H., Wang, R., Augusto, L., Lun, F.,
376 Nesme, T., Borrelli, P., Helfenstein, J., McDowell, R. W., Pletnyakov, P., and Pellerin, S.: A global dataset on phosphorus in
377 agricultural soils, *Scientific Data* 2024 11:1, 11, 1–34, https://doi.org/10.1038/s41597-023-02751-6, 2024.

378 Robertson, D. M. and Saad, D. A.: Spatially referenced models of streamflow and nitrogen, phosphorus, and suspended-
379 sediment loads in streams of the midwestern United States, https://doi.org/10.3133/sir20195114, 2019.

380 Royer, T. V., David, M. B., and Gentry, L. E.: Timing of riverine export of nitrate and phosphorus from agricultural watersheds
381 in Illinois: Implications for reducing nutrient loading to the Mississippi River, *Environ Sci Technol*, 40, 4126–4131,
382 https://doi.org/10.1021/ES052573N/ASSET/IMAGES/LARGE/ES052573NF00004.JPG, 2006a.



383 Royer, T. V., David, M. B., and Gentry, L. E.: Timing of Riverine Export of Nitrate and Phosphorus from Agricultural
384 Watersheds in Illinois: Implications for Reducing Nutrient Loading to the Mississippi River, *Environ Sci Technol*, 40, 4126–
385 4131, <https://doi.org/10.1021/es052573n>, 2006b.

386 Runkel, R. L., Crawford, C. G., and Cohn, T. A.: Load Estimator (LOADEST): A FORTRAN program for estimating
387 constituent loads in streams and rivers, <https://doi.org/10.3133/tm4A5>, 2004.

388 Sabo, R. D., Clark, C. M., Gibbs, D. A., Metson, G. S., Todd, M. J., LeDuc, S. D., Greiner, D., Fry, M. M., Polinsky, R., Yang,
389 Q., Tian, H., and Compton, J. E.: Phosphorus Inventory for the Conterminous United States (2002–2012), *J Geophys Res
390 Biogeosci*, 126, <https://doi.org/10.1029/2020JG005684>, 2021.

391 Sabo, R. D., Pickard, B., Lin, J., Washington, B., Clark, C. M., Compton, J. E., Pennino, M., Bierwagen, B., LeDuc, S. D.,
392 Carleton, J. N., and others: Comparing drivers of spatial variability in US lake and stream phosphorus concentrations, *J
393 Geophys Res Biogeosci*, 128, e2022JG007227, 2023.

394 Singh, N. K., Van Meter, K. J., and Basu, N. B.: Widespread increases in soluble phosphorus concentrations in streams across
395 the transboundary Great Lakes Basin, *Nature Geoscience* 2023 16:10, 16, 893–900, [https://doi.org/10.1038/s41561-023-01257-5](https://doi.org/10.1038/s41561-023-
396 01257-5), 2023.

397 Skinner, K. D. and Maupin, M. A.: Point-source nutrient loads to streams of the conterminous United States, 2012, Data Series,
398 <https://doi.org/10.3133/DS1101>, 2019.

399 Stackpoole, S. M., Stets, E. G., and Sprague, L. A.: Variable impacts of contemporary versus legacy agricultural phosphorus
400 on US river water quality, *Proc Natl Acad Sci U S A*, 116, 20562–20567,
401 https://doi.org/10.1073/PNAS.1903226116/SUPPL_FILE/PNAS.1903226116.SAPP.PDF, 2019.

402 Understanding phosphorus: global challenges and solutions: [https://www.unep.org/news-and-stories/story/what-phosphorus-
and-why-are-concerns-mounting-about-its-environmental-impact](https://www.unep.org/news-and-stories/story/what-phosphorus-
403 and-why-are-concerns-mounting-about-its-environmental-impact), last access: 26 February 2025.

404 Wang, F., Li, S., Yan, W., Yu, Q., Tian, S., Yan, J., Zhou, D., and Shao, Y.: Dependence of riverine total phosphorus retention
405 and fluxes on hydrology and river size at river network scale, *J Hydrol (Amst)*, 652, 132676,
406 <https://doi.org/10.1016/j.jhydrol.2025.132676>, 2025.

407 Wang, Y., Zhang, X., and Zhao, K.: A dataset of riverine nitrogen yield across watersheds in the Conterminous United States,
408 *Scientific Data* 2024 11:1, 11, 1–8, <https://doi.org/10.1038/s41597-024-03552-1>, 2024a.

409 Wang, Y., Zhang, X., Zhao, K., and Singh, D.: Streamflow in the United States: Characteristics, trends, regime shifts, and
410 extremes, *Sci Data*, 11, 788, <https://doi.org/10.1038/s41597-024e-03618-0>, 2024b.

411 Wang, Y., Zhang, X., Zhao, K., Sabo, R., Miao, Y., and Clark, C.: Riverine Phosphorus Gain and Loss across the conterminous
412 United States, *Figshare*, [data set], <https://doi.org/10.6084/m9.figshare.28509317>, 2025.

413 Wilson, D. J.: The harmonic mean p -value for combining dependent tests, *Proceedings of the National Academy of Sciences*,
414 116, 1195–1200, <https://doi.org/10.1073/pnas.1814092116>, 2019.

415 Withers, P. J. A. and Jarvie, H. P.: Delivery and cycling of phosphorus in rivers: A review, *Science of The Total Environment*,
416 400, 379–395, <https://doi.org/10.1016/j.scitotenv.2008.08.002>, 2008.



417 Wurtsbaugh, W. A., Paerl, H. W., and Dodds, W. K.: Nutrients, eutrophication and harmful algal blooms along the freshwater
418 to marine continuum, *WIREs Water*, 6, <https://doi.org/10.1002/wat2.1373>, 2019.

419 Xia, Y., Zhang, M., Tsang, D. C. W., Geng, N., Lu, D., Zhu, L., Igalavithana, A. D., Dissanayake, P. D., Rinklebe, J., Yang,
420 X., and Ok, Y. S.: Recent advances in control technologies for non-point source pollution with nitrogen and phosphorous from
421 agricultural runoff: current practices and future prospects, *Appl Biol Chem*, 63, 8, <https://doi.org/10.1186/s13765-020-0493-6>, 2020.

422 Zhang, Q. and Hirsch, R. M.: River Water-Quality Concentration and Flux Estimation Can be Improved by Accounting for
423 Serial Correlation Through an Autoregressive Model, *Water Resour Res*, 55, 9705–9723,
424 <https://doi.org/10.1029/2019WR025338>, 2019.

425 Zhang, W., Jin, X., Liu, D., Lang, C., and Shan, B.: Temporal and spatial variation of nitrogen and phosphorus and
426 eutrophication assessment for a typical arid river — Fuyang River in northern China, *Journal of Environmental Sciences*, 55,
427 41–48, <https://doi.org/10.1016/J.JES.2016.07.004>, 2017.

428

429

430